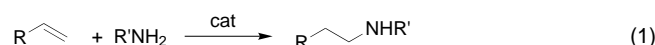


- Tolman, F. E. Romesberg, P. G. Shultz, *J. Am. Chem. Soc.* **2000**, *122*, 10714–10715.
- [5] Three reports have described systems containing branched/difunctional oligonucleotides and metal centers; however, none of these systems has a metal center whose geometry directly influences the orientation of the DNA strands. a) S. Takenaka, Y. Funatu, H. Kondo, *Chem. Lett.* **1996**, 891–892; b) F. D. Lewis, S. A. Helvoigt, R. L. Letsinger, *Chem. Commun.* **1999**, 327–328; c) see ref. [2g].
- [6] a) K. B. Reddy, M. P. Cho, J. F. Wishart, T. J. Emge, S. S. Isied, *Inorg. Chem.* **1996**, *35*, 7241–7245; b) T. Pascher, J. R. Winkler, H. B. Gray, *J. Am. Chem. Soc.* **1998**, *120*, 1102–1103.
- [7] M. J. Damha, K. Ganeshan, R. H. E. Hudson, S. V. Zabarylo, *Nucleic Acids Res.* **1992**, *24*, 6565–6573.
- [8] Selected spectroscopic data of complex **2**:  $^1\text{H}$  NMR (400 MHz,  $[\text{D}_6]\text{acetone}$ ):  $\delta = 0.85$  (m, 4H), 1.10 (m, 4H), 1.25 (m, 4H), 1.55 (m, 4H), 3.30 (t, 4H), 3.90 (t, 4H), 6.80 (s, 2H), 7.18 (brs, 2H), 7.32 (t, 2H), 7.72 (t, 2H), 7.82 (brs, 2H), 7.89 (t, 2H), 8.10 (m, 4H), 8.45 (d, 2H), 8.54 (d, 2H), 9.13 (d, 2H). FAB-MS:  $m/z$ : 894.9  $[M - \text{PF}_6]$ .
- [9] a) K. Iizuka, K. Akahane, Y. Kamijo, D. Momose, Y. Ajisawa, *Brit. UK Pat. Appl.* **1979**, GB2016452; b) G. M. Brown, R. W. Callahan, T. J. Meyer, *Inorg. Chem.* **1975**, *14*, 1915–21.
- [10] The expected diastereomers from the chirality of both the  $\text{cis}[(\text{bpy})_2\text{Ru}(\text{imidazole})_2]^{2+}$  and the phosphoramidite groups could not be resolved at 200 MHz.
- [11] Complex **1**: HPLC: 22% of the mixture, MALDI-TOF MS:  $m/z$ : 6861  $[M+2\text{Na}^+]$ . Complex **4**: HPLC: 54% of the mixture, MALDI-TOF MS:  $m/z$ : 3914  $[M+2\text{Na}^++\text{Li}^+]$ .
- [12] The buffer system used was 140 mM KCl, 5 mM  $\text{Na}_2\text{HPO}_4$ , and 1 mM  $\text{MgCl}_2$ , pH 7.2. This buffer is known to inhibit the formation of a DNA triple helix, which could arise from the association of **1** with one strand of  $\text{dA}_{10}$ .<sup>[14]</sup>
- [13] In parallel, control experiments on complex **2** established that the  $\text{cis}[(\text{bpy})_2\text{Ru}(\text{imidazole})_2]^{2+}$  moiety is stable to the high temperatures required in the melting experiments.
- [14] The origin of the observed increase in stability of the duplexes in **5**, as compared to natural  $\text{dA}_{10}/\text{dT}_{10}$  duplexes, is still under investigation. Thermal denaturation studies on monostranded complex **4** with  $\text{dA}_{10}$  showed a similar increase in  $T_m$ ,<sup>[17]</sup> and this suggests that the enhanced stability of the DNA duplexes in these structures may be due to the positively charged metal center. In this respect, the decrease in  $T_m$  and hyperchromicity observed for complex **1** with 1 equiv of  $\text{dA}_{10}$  relative to 2 equiv  $\text{dA}_{10}$  is also under investigation.
- [15] Assuming B-form DNA and fixing the coordinates of the ruthenium moiety according to a reported crystal structure of  $\text{cis}[(\text{bpy})_2\text{Ru}(\text{imidazole})_2]^{2+}$ ,<sup>[6a]</sup> calculations were performed with Hyperchem 6, Hypercube, FL (USA).
- [16] Current efforts are focused on the synthesis of analogues of **1** with rigid spacers between imidazole ligands and DNA strands, so that the geometry of the metal center can directly influence the orientation of the strands.
- [17] See Supporting Information for experimental details on the synthesis and characterization of complexes **1–4**, as well as thermal denaturation studies.

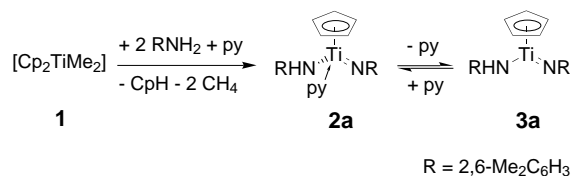
## The Mechanism of Hydroamination of Allenes, Alkynes, and Alkenes Catalyzed by Cyclopentadienyltitanium–Imido Complexes: A Density Functional Study\*\*

Bernd F. Straub\* and Robert G. Bergman\*

Considerable effort has been directed towards the development of procedures for hydroamination across carbon–carbon multiple bonds, and several catalytic systems for allene, alkyne, and alkene hydroamination have been investigated.<sup>[1]</sup> However, a general catalyst for the hydroamination of nonactivated unsaturated hydrocarbons remains elusive. A catalyst for the selective anti-Markovnikov addition of amines to terminal alkenes would be of particular interest [Eq. (1)].



Recent kinetic studies have been carried out to elucidate the mechanism of hydroamination catalyzed by cyclopentadienyltitanium complexes<sup>[2–5]</sup> such as the dimethyltitanocene **1** and the imido complex **2a** (Scheme 1).<sup>[4,5]</sup> Formation of the active monocyclopentadienyltitanium–imido species  $[\text{CpTi}=\text{NR}(\text{NHR})]$  **3a** ( $\text{R} = 2,6\text{-Me}_2\text{C}_6\text{H}_3$ ) from both the pyridine adduct **2a** and the precatalyst **1** has been established (Scheme 1).<sup>[4]</sup>



Scheme 1. Generation of  $[\text{CpTi}=\text{NR}(\text{NHR})]$  **3a** from precatalyst  $[\text{Cp}_2\text{TiMe}_2]$  (**1**) and by equilibration with  $[\text{CpTi}=\text{NR}(\text{NHR})\text{py}]$  **2a**.<sup>[4]</sup>

Titanaazacyclobutenes and titanaazacyclobutanes are proposed as intermediates in the catalytic cycle,<sup>[2a,4,5]</sup> in analogy to the  $[\text{Cp}_2\text{Zr}(\text{NHR})_2]$ -catalyzed hydroamination of alkynes<sup>[6]</sup> or the stoichiometric reaction of allenes with zirconium and titanium pyridine imido derivatives.<sup>[7]</sup> However, the mechanism of the protonation of the titanacycle by the amine is not well understood. Here we report high-level density functional model calculations on the intermediates involved in this step. The origin of the differences between the activation barriers

[\*] Dr. B. F. Straub, Prof. R. G. Bergman  
Department of Chemistry  
University of California  
Berkeley, CA 94720-1460 (USA)  
Fax: (+1) 510-642-7714  
E-mail: bergman@cchem.berkeley.edu  
bfstraub@uclink.berkeley.edu

[\*\*] This work was supported by the US National Institutes of Health (grant no. GM-25459 to R.G.B.). B.F.S. gratefully acknowledges a Feodor Lynen research fellowship of the Alexander von Humboldt foundation.

Supporting information for this article is available on the WWW under <http://www.angewandte.com> or from the author.

in allene and alkyne versus the hypothetical alkene hydroamination catalysis is also explored.

We used the B3LYP functionals,<sup>[8]</sup> a Hay–Wadt small-core effective-core potential on titanium,<sup>[9]</sup> and a triple- $\zeta$  plus polarization quality basis set<sup>[10]</sup> for geometry optimization and vibrational frequency analyses.<sup>[11]</sup> Since total electronic energies are not sufficient for the prediction of barriers for association and dissociation reactions at room or elevated temperature, zero-point vibrational energies and Gibbs free energy corrections have been included for all simplified compounds.

In earlier experimental studies on allene hydroamination, our group observed a first-order dependence on the concentration of catalyst **2a** and allene substrate, a zero-order dependence on the 2,6-dimethylaniline concentration, and an inverse first-order rate dependence on the pyridine concentration.<sup>[4]</sup> The pyridine adduct **2a** is stable in the presence of 2,6-dimethylaniline towards formation of species such as  $[\text{CpTi}(\text{NHR})_3]$  (**4a**), dinuclear complexes such as **5a**, and free pyridine.<sup>[4]</sup> Pohlki and Doye observed that the rate of diphenylacetylene hydroamination depends on both the concentration of precatalyst **1** and 4-methylaniline.<sup>[5]</sup> Their kinetic analysis postulated the existence of preequilibria that interconvert the active imido species with both titanium amides and dinuclear titanium complexes,<sup>[5]</sup> and this also explains the low reaction rates of sterically less hindered amines.<sup>[3]</sup>

We first studied the relative energies of potential catalyst resting states. The preference for pyridine ligation is indeed reproduced by the DFT calculations in the nonsimplified models **2a–5a** (Figure 1).

Although the computed strength of pyridine coordination to the simplified  $\{\text{CpTi}=\text{NH}(\text{NH}_2)\}$  fragment in **2b** is weaker than the driving force for formation of trisamide **4b** and dimer **5b**, the steric congestion of three 2,6-dimethylanilide ligands at a titanium center inverts the relative stabilities. The computed steric influence of the amine substituents for the stabilities of the titanium species **3** to **5** strongly supports the interpretations of the Doye group.<sup>[5]</sup>

Next we studied the interaction of these titanium complexes with unsaturated hydrocarbons. The presumed active species **3b** weakly coordinates to allene (Figure 2), ethyne

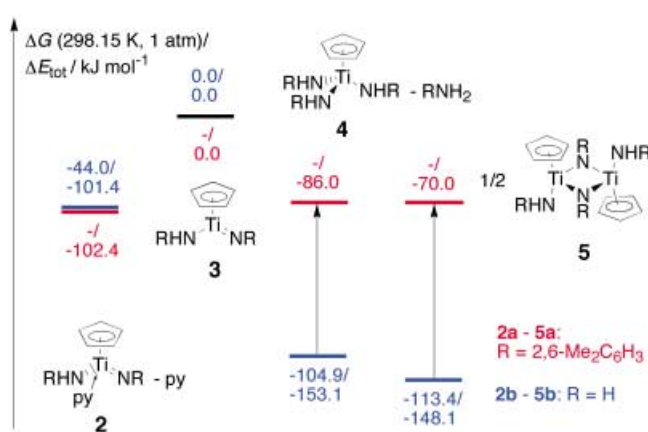


Figure 1. Influence (see arrows) of the amide and imide substituents on the computed relative stabilities of CpTi complexes.

(Figure 3), or ethene (Figure 4), and is predicted to undergo a facile  $[2+2]$  cycloaddition with each substrate.

Two pathways for the overall hydroamination reaction have been found for each of the hydrocarbon substrates.

- 1) Coordination of  $\text{NH}_3$  and intramolecular proton transfer from the ammine ligand to a carbon atom (Figure 2 to 4).
- 2) Proton transfer from an amide ligand to a carbon atom without preceding amine coordination (Figure 5).

The coordination of  $\text{NH}_3$  in **11**, **17**, and **23** acidifies the ammine protons compared to those of free ammonia. This is reflected in NBO analyses, which reveal a charge transfer of  $-0.22$  to  $-0.24$  from the ammine ligand to the titanium fragment and a concomitant increase in negative net charge on the C1 carbon atom.<sup>[12]</sup>

In both the allene and the ethyne pathways, the presence of a vinylamine-type  $\pi$  system facilitates proton transfer. In the allene hydroamination cycle, a proton on the ammine ligand is transferred to the *exo*-methylene group. In a concerted reaction, the Ti–C3 bond cleaves (2.226 Å in **11**, 2.369 Å in **12**), the C1–C2 double bond character vanishes (1.358 Å in **11**, 1.421 Å in **12**), and a C2–C3 double bond is formed (1.475 Å in **11**, 1.426 Å in **12**; see Figure 2 and 3). In the ethyne pathway, coordination of  $\text{NH}_3$  distorts the titanazacyclobutene (**17**) ( $\delta(\text{Ti}-\text{C}1-\text{C}2-\text{N}1)=29.5^\circ$ , see Figure 3). The

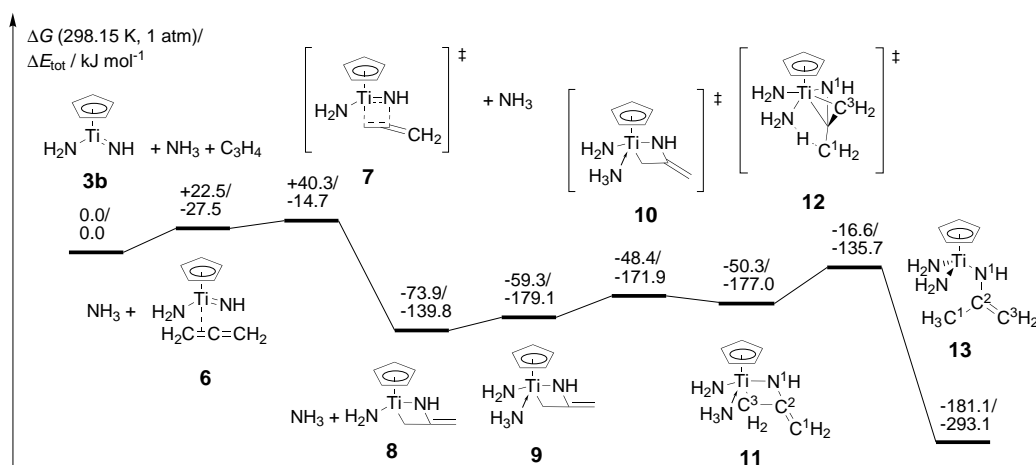


Figure 2. Allene hydroamination pathway:  $[2+2]$  cycloaddition,  $\text{NH}_3$  coordination, ring inversion via **10**, and intramolecular proton transfer.

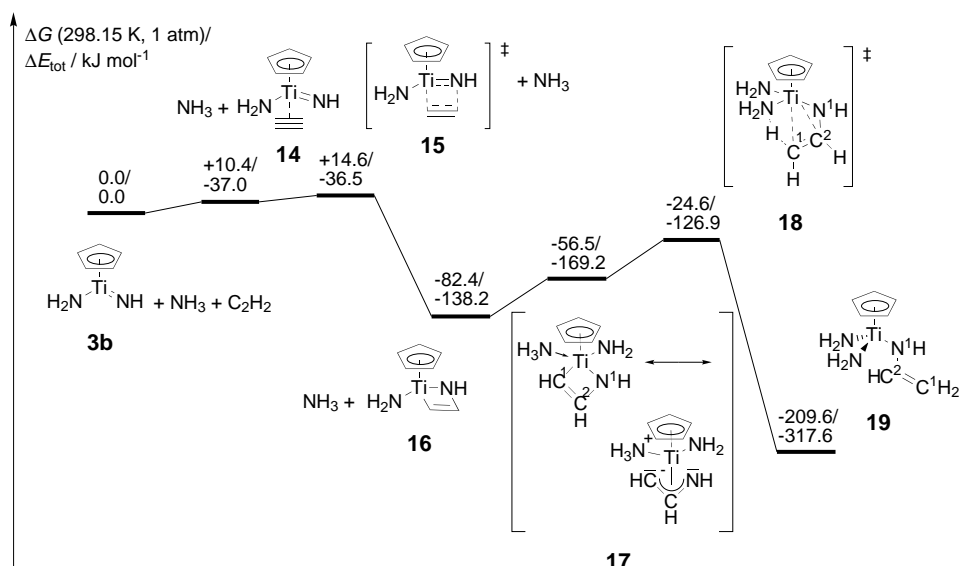


Figure 3. Ethyne hydroamination pathway: [2+2] cycloaddition, NH<sub>3</sub> coordination, and proton transfer.

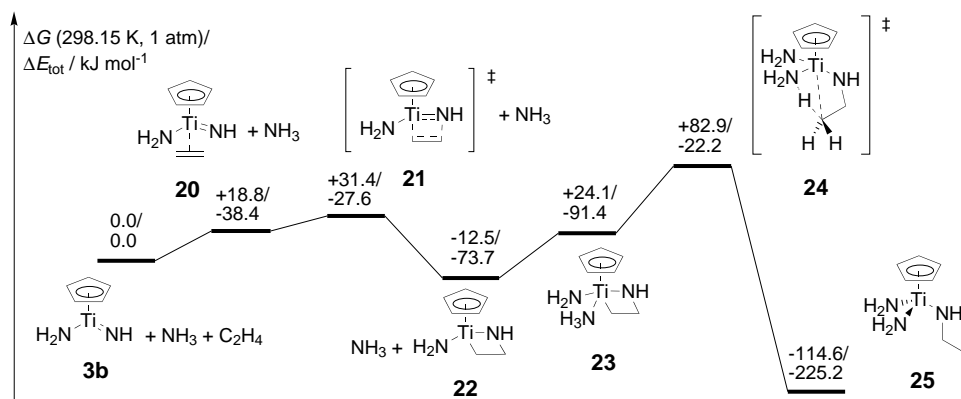


Figure 4. Hypothetical ethene hydroamination pathway: [2+2] cycloaddition, NH<sub>3</sub> coordination, and proton transfer.

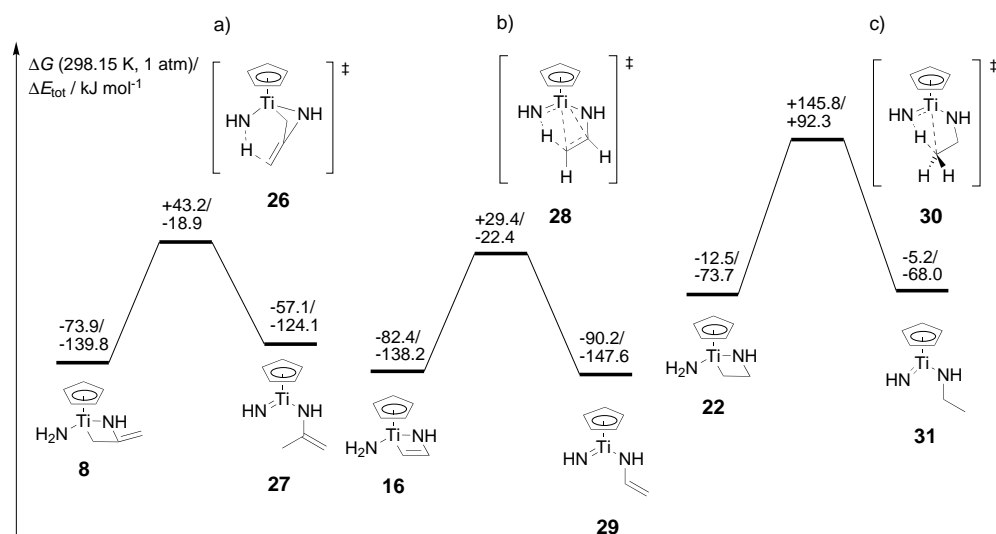


Figure 5. Alternative mechanistic pathways for proton transfer from an amide ligand: hydroamination of (a) allene, (b) ethyne, and (c) ethene.

resulting contribution of a mesomeric structure with a deprotonated dianionic  $\eta^3$ -1-azaallyl ligand facilitates the proton transfer. As in the allene hydroamination pathway, the Ti–C bond is cleaved as the proton transfer proceeds (Figure 3).

We next studied the hypothetical ethene hydroamination. The Gibbs free dissociation energy of ethene from titanacycle **22** is computed to be more than 60 kJ mol<sup>-1</sup> lower than for the corresponding allene or ethyne dissociation reaction. The NH<sub>3</sub> addition to the ethene adduct **22** is slightly disfavored by 10 to 15 kJ mol<sup>-1</sup> compared to the NH<sub>3</sub> addition to the allene and ethyne analogues **11** and **17** (Figure 4). Furthermore, no  $\pi$  system is present in the titanacycle **23** and thus the  $\sigma$  Ti–C bond has to be directly protonated. As a consequence, the proton transfer is disfavored by an additional 25 to 30 kJ mol<sup>-1</sup>. Altogether, the proton transfer step in alkene hydroamination by CpTi–imido complexes is disfavored by about 100 kJ mol<sup>-1</sup> compared to the corresponding allene and alkyne proton transfer steps.

Since the ammine complexes and their proton transfer transition states possess the highest coordination number at the respective titanium center in the catalytic cycle, they are especially sensitive to steric congestion. As a consequence, bulky amines and sterically demanding unsaturated substrates might support an electronically disfavored and entropically favored pathway without precoordination of amine, but rather with direct proton transfer from an amide ligand to a carbon atom. The computed energetics for these pathways are shown in Figure 5.

The predicted increase in electronic barriers for the amide protonation transfer

compared to the barriers for the respective ammine proton transfer reactions results from the increased distortion of the core structures in the transition states and the lower acidity of the amide protons. Zero point vibration and entropic contributions lower the Gibbs free energy barrier difference between the two pathways to 54–63 kJ mol<sup>-1</sup> by destabilizing the highly ordered ammine proton transfer transition states **12**, **18**, and **24**. This difference could well be overcome by steric congestion induced by bulky substituents of amines and unsaturated hydrocarbon substrates. For comparison, the steric destabilization for complexes with three 2,6-dimethylanilide ligands at a titanium center such as in **4a** and **5a** has been computed to be 67–78 kJ mol<sup>-1</sup>.

In allene and ethyne hydroamination with the simplified [CpTi=NH(NH<sub>2</sub>)] system, where proton transfer takes place after initial amine coordination, the transition state for the cycloaddition is the highest point in the catalytic pathway and thus is rate-determining. However, it remains unclear whether the zero-order dependence on the 2,6-dimethylaniline concentration derived from the kinetic data for allene hydroamination<sup>[4]</sup> results from a rate-determining [2+2] cycloaddition or a rate-determining proton transfer from an amide ligand. A first-order dependence on the amine concentration can occur if the Gibbs free activation energy for the amine coordination plus proton transfer pathway is higher than the barrier for the initial [2+2] cycloaddition, but lower than the barrier for a competing amide proton transfer. A rate-determining amide ligand exchange with free amine could also result in such a rate law (see Supporting Information for computed ligand exchange pathways).

For alkene hydroamination, our model calculations predict that both the ammine and the amide proton transfer to the Ti–C bond have Gibbs free activation energies that are more than 50 kJ mol<sup>-1</sup> higher than the cycloaddition step (Figure 4 and 5c). This explains the relative ease of allene and alkyne hydroamination compared to alkene hydroamination. Increasing the rate of this proton transfer step as well as stabilizing the metallazaacyclobutane intermediate compared to the catalyst resting state could be the key to making the alkene process successful. We are using these new insights into the hydroamination mechanism to isolate additional intermediates involved in the catalytic cycle, and to tailor more general hydroamination catalysts.

Received: August 9, 2001

Revised: October 5, 2001 [Z17699]

- [1] a) T. E. Müller, M. Beller, *Chem. Rev.* **1998**, *98*, 675, and references therein; b) M. Tokunaga, M. Eckert, Y. Wakatsuki, *Angew. Chem.* **1999**, *111*, 3416; *Angew. Chem. Int. Ed.* **1999**, *38*, 3222; c) H. M. Senn, P. E. Blöchel, A. Togni, *J. Am. Chem. Soc.* **2000**, *122*, 4098; d) M. Kawatsura, J. F. Hartwig, *J. Am. Chem. Soc.* **2000**, *122*, 9546; e) M. Kawatsura, J. F. Hartwig, *Organometallics* **2001**, *20*, 1960; f) O. Löber, M. Kawatsura, J. F. Hartwig, *J. Am. Chem. Soc.* **2001**, *123*, 4366; g) H. Schaffrath, W. Keim, *J. Mol. Catal. A* **2001**, *168*, 9; h) M. Nobis, B. Drießen-Hölscher, *Angew. Chem.* **2001**, *113*, 4105; *Angew. Chem. Int. Ed.* **2001**, *40*, 3983.
- [2] a) P. L. McGraine, M. Jensen, T. Livinghouse, *J. Am. Chem. Soc.* **1992**, *114*, 5459; b) P. L. McGrane, T. Livinghouse, *J. Am. Chem. Soc.* **1993**, *115*, 11485; c) P. L. McGrane, T. Livinghouse, *J. Org. Chem.* **1992**, *57*, 1323.

- [3] a) E. Haak, I. Bytchow, S. Doye, *Angew. Chem.* **1999**, *111*, 3584; *Angew. Chem. Int. Ed.* **1999**, *38*, 3389; b) E. Haak, H. Siebeneicher, S. Doye, *Org. Lett.* **2000**, *2*, 1935.
- [4] J. S. Johnson, R. G. Bergman, *J. Am. Chem. Soc.* **2001**, *123*, 2923.
- [5] F. Pohki, S. Doye, *Angew. Chem.* **2001**, *113*, 2361; *Angew. Chem. Int. Ed.* **2001**, *40*, 2305.
- [6] a) P. J. Walsh, A. M. Baranger, R. G. Bergman, *J. Am. Chem. Soc.* **1992**, *114*, 1708; b) A. M. Baranger, P. J. Walsh, R. G. Bergman, *J. Am. Chem. Soc.* **1993**, *115*, 2753.
- [7] a) Z. K. Sweeney, J. L. Salsman, R. A. Andersen, R. G. Bergman, *Angew. Chem.* **2000**, *112*, 2429; *Angew. Chem. Int. Ed.* **2000**, *39*, 2339; b) A. Bashall, M. McPartlin, P. E. Collier, P. Mountford, L. H. Gade, D. J. M. Troesch, *Chem. Commun.* **1998**, 2555; c) D. J. M. Troesch, P. E. Collier, A. Bashall, L. H. Gade, M. McPartlin, P. Mountford, S. Radojevic, *Organometallics* **2001**, *20*, 3308.
- [8] a) A. D. Becke, *J. Chem. Phys.* **1993**, *98*, 5648; b) S. H. Volko, L. Wilk, M. Nusair, *Can. J. Phys.* **1980**, *58*, 1200; c) C. Lee, W. Yang, R. G. Parr, *Phys. Rev. B* **1988**, *37*, 785.
- [9] R. Krishnan, J. S. Binkley, R. Seeger, J. Pople, *J. Chem. Phys.* **1980**, *72*, 650.
- [10] P. J. Hay, W. R. Wadt, *J. Chem. Phys.* **1985**, *82*, 299.
- [11] Jaguar 4.0, release 23, Schrödinger, Inc., Portland, OR, USA, **1998**.
- [12] NBO net charge of the hydrogen atoms of NH<sub>3</sub>: 0.338; NBO net charge of the hydrogen atoms of the ammine ligand of **11**: 0.386 to 0.414; **17**: 0.379 to 0.402, **23**: 0.383 to 0.389. NBO 4.0. E. D. Glendening, J. K. Badenhoop, A. E. Reed, J. E. Carpenter, F. Weinhold, Theoretical Chemistry Institute, University of Wisconsin, Madison, WI, **1999**.

## Self-Assembly of Cyclic Peptides into Nanotubes and Then into Highly Anisotropic Crystalline Materials\*\*

David Gauthier, Pierre Baillargeon, Marc Drouin, and Yves L. Dory\*

Syntheses of supermolecules rely on the stabilization provided by noncovalent interactions between recognition sites in each unit.<sup>[1–3]</sup> The construction of new supramolecular architectures with well-defined shape and size by using tube building blocks is an important subject in organic materials chemistry because novel electronic and photonic properties can result from their three-dimensional (3D) organization (Figure 1a).<sup>[2]</sup> These tubular structures have also attracted considerable interest because of their utility as models for biological channels.<sup>[4–9]</sup> It is also thought that in tubes built from stacked cyclic peptides, uniform alignment of amide groups could give rise to a macrodipole moment such as that of an  $\alpha$ -helix.<sup>[10]</sup> Voltage gating and current rectification are important expected new properties for such channel structures.<sup>[11]</sup>

To date, all attempts to grow crystals of a useful size were frustrated by the inherent insolubility of these materials.<sup>[12–15]</sup>

[\*] Prof. Y. L. Dory, D. Gauthier, P. Baillargeon, M. Drouin  
Laboratoire de Synthèse Supramoléculaire, Département de Chimie  
Université de Sherbrooke  
3001 12e Avenue nord, Fleurimont, J1H 5N4, PQ (Canada)  
Fax: (+1) 819-820-6823  
E-mail: yves.dory@courrier.usherb.ca

[\*\*] This work was supported by FCAR Québec.